

Negative Capacitance Phenomenon in GaAs-Based MIS Devices Under Ionizing Radiation

Ahmet Kaymaz

Abstract— This study focuses on the abnormal peaks observed in voltage-dependent capacitance graphs and negative capacitance behaviours of the GaAs-based MIS devices for the unirradiated sample and after exposing the device to 5 and 10 kGy ionizing (gamma) radiation doses. Experimental results showed that the amplitude of the abnormal peaks, observed at about 1.75 V, increases with the irradiation dose. The peak point was also shifted toward the positive biases after irradiation. Furthermore, the conductance values increased rapidly and reached their maximum level, while the capacitance values reached their minimum level in the high voltage biases. It is known that this situation is directly related to the inductive behaviour of the MIS devices. However, it has been determined that the MIS device's inductive behaviour is more effective after irradiation. These behaviours can be observed because of the ionization process, the MIS device's series resistance, surface states, and due to some displacement damages caused by ionizing radiation. Therefore, the series resistance and the radiation-induced surface states were obtained to clarify the impact of radiation on the device. It was seen that the radiation-induced surface states changed around $3 \times 10^{12} \text{ eV}^{-1} \text{ cm}^{-2}$ for the maximum cumulative dose (10 kGy), and the series resistance values changed to less than 2Ω . As a result, the degradation in the GaAs-based MIS device was determined to be insignificant for 10 kGy doses. Therefore, this MIS device can be safely used as an electronic component in radiation environments such as nuclear plants and satellite systems.

Index Terms— Abnormal/Anomalous peak, GaAs-based devices, Ionizing radiation, MIS devices, Negative capacitance.

I. INTRODUCTION

IT IS KNOWN THAT Schottky diodes/structures are obtained by contacting metal and semiconductor (M/S) materials with or without oxide/insulator or ferroelectric interlayers [1]. These structures are also the basis of many electronic devices, such as photodiodes, photodetectors, transistors, and solar cells [2]. Interfacial layers can be grown between the M/S interface by native or some special methods [3]–[5]. Many ways are used to deposit an interfacial layer, such as the sol-gel method [6], [7], chemical vapour


deposition [8], electrospinning [9], [10], molecular beam layer deposition [11], and spin coating [12] as well as other techniques [13]. In this study, the oxide layer was grown by a natural method due to the stable behaviour of the Si and SiO₂ combination [5]. The oxide interlayer also controls interdiffusions between the M/S interface and prevents possible chemical reactions. Furthermore, the devices can gain better capacitive features due to the dielectric effect of the oxide interfacial layer [14].

When the interfacial layer obtained using an oxide or an insulating material in the devices is thinner than 500 Å, this device can be used as a diode [15]. Such devices are referred to as Schottky diode/structure due to the critical works in this area proposed by W. H. Schottky. If the thickness of the oxide/insulator interlayer is greater than 500 Å, such a structure is defined as a capacitor rather than a diode. It is well-known that these devices cannot provide carrier conduction at the M/S interface and, therefore, can store electrical charges and energy [15], [16]. In this study, the thickness of the natural oxide layer for the Au/n-GaAs/Au-Ge type Schottky device was obtained as approximately 23.4 Å using Nicollian and Goetzberger calculation method [17]. Therefore, it can be defined as a metal-insulator-semiconductor (MIS) type Schottky diode or MIS device.

GaAs in the III-V semiconductor group have a wide-direct bandgap and high saturation velocity. GaAs-based designs are also high-speed and low-power consumption devices because of their high mobility, which is approximately six times higher than silicon [2], [18]. These properties make it highly suitable for fabricating M/S-type Schottky devices and make GaAs preferable as a semiconductor for high-power devices used at high frequencies [1], [19], [20]. On the other hand, it has been reported in some previous studies that GaAs-based devices are less affected by radiation damage than other devices [21]. Therefore, GaAs-based materials could be critical devices for future improvement technology. As a result, this study, which aims to understand the radiation impact of GaAs-based devices for attractive voltage regions, is crucial because of the need to reliably/safely use devices that can operate under radiation, such as biomedical devices and satellite systems or nuclear plant devices.

As well as optoelectronic applications [22], there are many reports on Schottky devices with various interfacial layers to obtain devices with better electrical and dielectric properties [23]–[28]. However, it is essential to investigate the ionizing radiation effects of such devices, especially GaAs-based devices, because of their superior features and interesting characteristic behaviours, especially at sufficient high positive voltages (accumulation region). When the voltage-dependent

AHMET KAYMAZ, is with Department of Mechatronics Engineering, Karabuk University, Karabük, Turkey (e-mail: ahmetkaymaz@karabuk.edu.tr).

 <https://orcid.org/0000-0003-2262-1599>

Manuscript received Nov 25, 2022; accepted Feb 23, 2023.

DOI: [10.17694/bajece.1210121](https://doi.org/10.17694/bajece.1210121)

capacitance (C - V) characteristics of GaAs-based devices are examined at sufficiently forward biases, it becomes possible to encounter negative capacitance values in this voltage region. Negative capacitance phenomenon can occur because of the series resistance, surface states, and minority carrier injection [29], [30]. The relaxation times of the surface states can also affect negative capacitance behaviour depending on frequency [31], [32]. On the other hand, some advantages of the negative capacitance effect in ferroelectric materials and the advantages of this effect have become an important topic in recent years [33]. And many studies have been carried out on these subjects [29]–[34]. However, the ionizing radiation effects of such devices have not been adequately studied, especially in sufficient forward biases where negative capacitance values are observed. Therefore, it is predictable that this study can significantly contribute to the literature to understand the device's radiation dependency, which has negative capacitance and anomalous/abnormal peak behaviour.

The type and dose of the ionizing radiation can affect the devices' electrical, optoelectronic, and dielectric features [28]. Many energetic particles, such as neutrons, alpha, and beta, as well as electromagnetic radiations, such as X and γ rays, are in the category of ionizing radiation. These high energy sources (ionizing radiation sources), which emit energetic photons of approximately 1 MeV, can cause events called displacement damage in electronic devices [35]. Displacement damage, defined as the separation of atoms from the standard lattice regions in the target material, can lead to new energy levels formation in the semiconductor band gap. Briefly stated, displacement damage caused by ionizing radiations leads to considerable changes in devices' electrical, optoelectronic, and dielectric features, which makes the reliability of devices used in radiation environments questionable. Therefore, the radiation effects of the electronic devices which possible use under ionizing radiation needs to be carefully studied and understood. The best way to understand these effects is to examine the device's voltage-dependent capacitance-conductance (C - G/ω - V) characteristics and other voltage-dependent current (I - V) characteristics. Since this study focuses on the negative capacitance behaviour with the abnormal peak phenomenon observed in C - V graphs, only the C - V and G/ω - V graphs of the GaAs-based MIS device have been discussed with some critical device parameters such as surface states (N_{ss}) and the series resistance (R_s).

II. MATERIALS AND METHODS

The fabrication processes of the GaAs-based with a natural oxide layer MIS device can be summarized in several primary stages. The first step is the chemical cleaning process applied to remove organic and metallic impurities from the surface of a (100) oriented n-type GaAs wafer. At this stage, the wafer was first degreased for about five minutes in some organic solvent mixtures well known in the literature and then etched several times in some solutions. At each step, the wafer was quenched in deionized water. Upon completion of the chemical cleaning process, it was quickly dried in a nitrogen gas environment.

In the second stage, before the formation of the ohmic contact, gold (Au) metal was doped with Ge to obtain a high-

quality ohmic contact [36]. Then the Au-Ge mixture (88% Au and 12% Ge) was evaporated onto the matte (back) surface of the n-type GaAs wafer in a high vacuum system. Afterwards, the n-GaAs/Au-Ge wafer was annealed at 450°C for about six-seven minutes in nitrogen ambient to reduce the ohmic contact resistivity, and 200 nm thick ohmic contact was obtained. Before proceeding to the Schottky contact process in the third stage of the production process, the wafer was kept in a clean room for a few days. Thus, the formation of a very thin natural oxide layer (≈ 2.3 nm) was allowed.

In the final stage of the production process, the Au metal with 99.999% purity was evaporated to the masked front surface of the n-type GaAs/Au-Ge wafer using the thermal metal evaporation system. Thus, many Schottky contacts with a thickness of 200 nm and an area of 7.85×10^{-3} cm² were obtained. So, the production process of the Au/(n-type GaAs)/Au-Ge with natural oxide layer (GaAs-based MIS devices) was completed. The schematic view of the produced GaAs-based MIS device can be seen in Fig. (1).

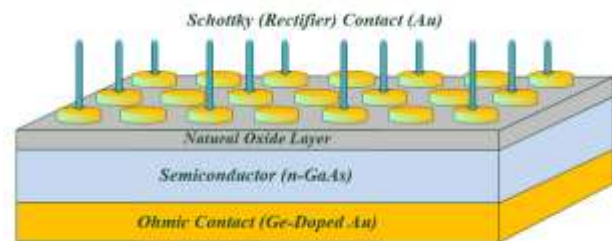


Fig.1. The representative view of the GaAs-based MIS device.

The GaAs-based MIS device's voltage-dependent capacitance and conductance values were obtained for the unirradiated sample (0 kGy) and after 5 and 10 kGy radiation doses for a wide voltage range (± 4 V) after the production process. The vpf-475 cryostat was used for measurements to rule out possible external influences, and Hewlett Packard Impedance Analyzer was used to obtain C - G/ω - V data. On the other hand, the Ob-Servo Sanguis ⁶⁰Co irradiation source located in Ankara was used to expose the devices to ionizing radiation (gamma rays). Detailed information for the measuring system can also be available [37]. The C - G/ω - V data for the unirradiated sample and after the irradiation processes were obtained at the high (500 kHz) frequency to eliminate fabrication-induced N_{ss} [38]. These measurements were carried out in the laboratory located at the Gazi University Photonics Application and Research Center.

III. RESULTS AND DISCUSSION

Some previous studies have shown that traps/charges can significantly change C - G/ω values, especially at low frequencies below 500 kHz, because they can easily track the ac signal [39]. However, at high frequencies ($f \geq 500$ kHz), these traps/loads cannot track the ac signal and therefore do not cause significant changes in C - G/ω values [31]. Another well-known fact is that the C - G/ω - V curves of the MIS/MOS devices are highly sensitive to ionizing radiation at high frequencies due to small capacitance/conductance values, mostly in the order of nF/pF. In addition, the disappearance of the effects of fabrication-induced surface conditions can be

shown as another reason for this situation. Therefore, the $C-G/\omega-V$ data obtained at high frequency can give us essential information about the radiation effects of the MIS devices.

The typical behaviour of the capacitance curves of an MIS/MOS device is given in the reference [40], and there are three regions, known in the literature as depletion, inversion, and accumulation regions, in these characteristics. Typical capacitance characteristics can also be divided into five areas: depletion (voltages around 0 V), weak accumulation-inversion (small positive-negative voltages), and strong accumulation-inversion (high positive-negative voltages) regions. The capacitance values in the high positive voltages can be considered almost independent of voltage in the ideal case. Their values also exhibit a curve behaviour almost independent of the frequency in the weak accumulation/inversion regions [41]. However, because of the surface states and accumulated charges, capacitance values can easily change depending on the frequency in the depletion region. It is known that the GaAs-based MIS devices' $C-V$ characteristics may exhibit negative behaviour or a concave curvature in the accumulation region due to the surface/dipole polarization, series resistance, and the interlayer growing between the M/S interface.

Voltage- and radiation-dependent $C-G/\omega-V$ curves given in Fig. (2) show that ionizing irradiation significantly affects the capacitance and conductance curves, especially in the accumulation and depletion regions. Besides, abnormal peak behaviours at about 1.75 V in the capacitance curves are striking for unirradiated measurements after each irradiation dose. On the other hand, all capacitance curves crossed at approximately 3.25 V, and these curves started to take negative values. It can also be seen in Fig. (2) that the peak point of the capacitance curves is shifted towards the positive voltages, and the amplitude of these peaks increases with the increase in gamma-ray amounts. These behaviours can be observed because of the ionization processes, the MIS device's series resistance, and surface states located between the M/S interface, as well as due to some effects (displacement damages) of ionizing radiation [29], [42]–[44].

The capacitance and conductance graphs show that while capacitance values decrease, conductance values increase with increasing biases in the high positive voltages. The conductance values also increase with increasing irradiation doses. Briefly stated, the conductance values increased rapidly and reached their maximum value, while the capacitance values reached their minimum value in the strong accumulation region. It is possible to say that this situation directly shows the inductive behaviour of the MIS devices. The behaviour of the negative capacitance values and increasing conductance values, depending on the increase in the radiation dose, also indicate that the inductive effect of the MIS device becomes more pronounced under ionizing radiation. Nevertheless, it is necessary to thoroughly examine the voltage-dependent resistance curves (R_f-V) and radiation-induced surface states to understand which parameter(s) cause these behaviours. Therefore, this issue should be reconsidered when discussing the R_f-V and radiation-dependent $N_{ss}-V$ graphs.

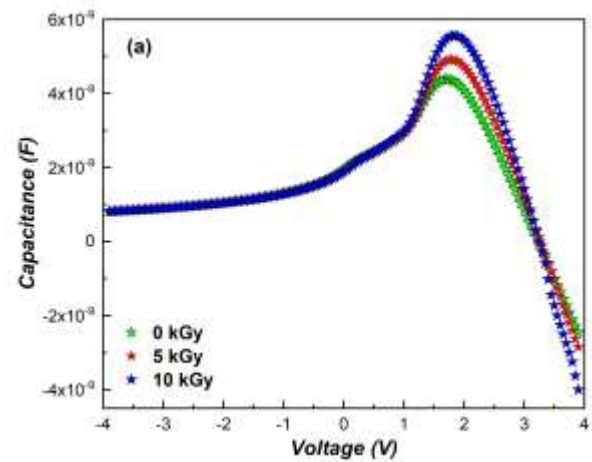


Fig.2a. The behaviour of the GaAs-based MIS device's capacitance curves under radiation.

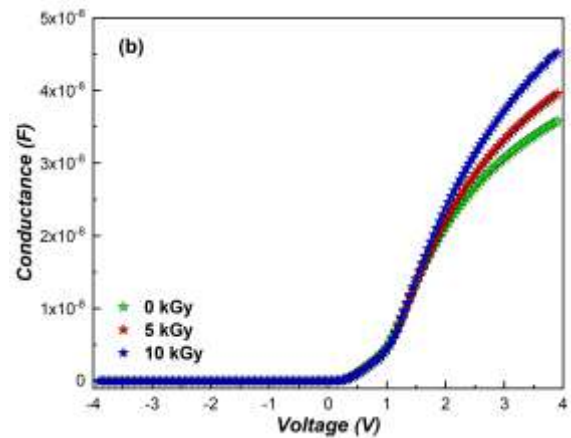


Fig.2b. The behaviour of the GaAs-based MIS device's conductance curves under radiation.

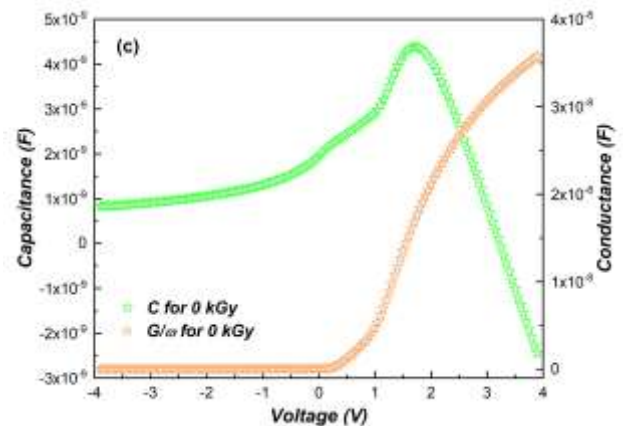


Fig.2c. The capacitance and conductance curves for the unirradiated sample.

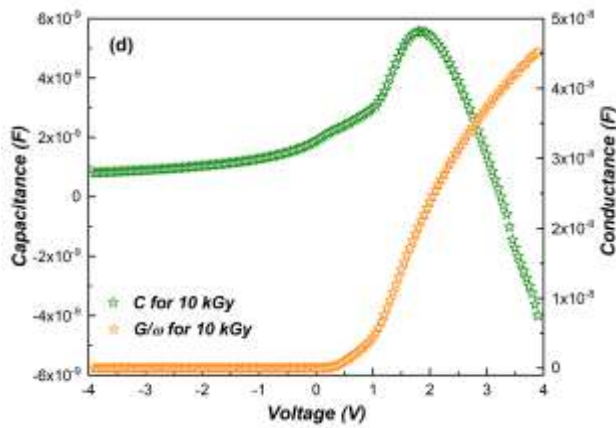


Fig.2d. The capacitance and conductance curves for 10 kGy radiation doses.

The Nicollian and Brews method ($R_i = G_m / [(G_m)^2 + (\omega C_m)^2]$) can be used in order to obtain R_i - V curves from the C - G/ω - V data, and so the actual series resistance values (R_s) for MIS devices can be determined from the high positive voltages of these curves [45]. Fig. (3), given R_i - V curves, shows that R_i values did not show a significant change depending on the radiation dose when viewed in terms of the curve shape in all regions. Besides, these curves showed peaks in the depletion region and remained almost constant in the high positive voltages where actual series resistance values are obtained. In brief, the R_s values vary as 8.74, 7.88, and 6.82 Ω for 0, 5, and 10 kGy ionizing (gamma) radiation doses.

Such a peak behaviour in R_i - V curves, thought to be due to the particular distribution of N_{ss} , has occurred in many devices [46]–[48]. However, due to the different effects of gamma irradiation on the devices, it has been determined that the series resistance values and peak amplitude may decrease or increase after the radiation process. The reduction in R_s values may be due to radiation defects and/or the annealing effect. On the other hand, the increasing behaviour is usually the result of the device's tendency to degrade under radiation. As a result, the reduction in R_s values under ionizing radiation of this MIS device is meagre and shows that the device is not prone to deterioration. Ionizing radiation changed the carrier mobility and free carrier concentration in the MIS device; therefore, a decrease in R_s values occurred. These effects have led to an increase in the conductance values in the high positive voltages.

In the previous paragraph, attention has been drawn to some resistance effects. However, it is necessary to obtain correct capacitance-conductance values (C_C - G/ω), which are eliminated R_s effects, and radiation-induced N_{ss} to determine all results of the series resistance on the behaviour of the device's electrical characteristics. It is known that the C_C and G/ω values can be obtained from Eqs. (1-3). Thus, the effects of R_s for each voltage region can be revealed. Therefore some graphs about the correct capacitance-conductance curves are obtained given in Figs. (5a-5d).

On the other hand, the high-low frequency method, which is used to calculate surface states, can also be used to obtain radiation-induced N_{ss} (provided in Eq. (4)) for all voltage biases [49]. Thus, the graphs of the radiation-induced N_{ss} that depend on voltage bias are determined and given in Fig. (4).

$$\alpha = G_m - [(G_m)^2 + (\omega C_m)^2] \times R_s \quad (1)$$

$$C_C = [(G_m)^2 + (\omega C_m)^2] \times C_m / [\alpha^2 + (\omega C_m)^2] \quad (2)$$

$$G_C = [(G_m)^2 + (\omega C_m)^2] \times \alpha / [\alpha^2 + (\omega C_m)^2] \quad (3)$$

$$N_{ss} = \left(\frac{1}{qA} \right) \times \left\{ \left(\frac{1}{C_{before}} - \frac{1}{C_{ox}} \right)^{-1} - \left(\frac{1}{C_{after}} - \frac{1}{C_{ox}} \right)^{-1} \right\} \quad (4)$$

Here, C_{before} represents the capacitance value of the unirradiated device, while C_{after} corresponds to the capacitance value of the irradiated sample at different doses. C_{ox} also corresponds to oxide layer capacitance. On the other hand, the interlayer capacitance (C_i) can be calculated from the C - G/ω - V data, and other parameters are also well-known in the literature ($C_i = [1 + (G/(\omega C))^2] \times C_m$).

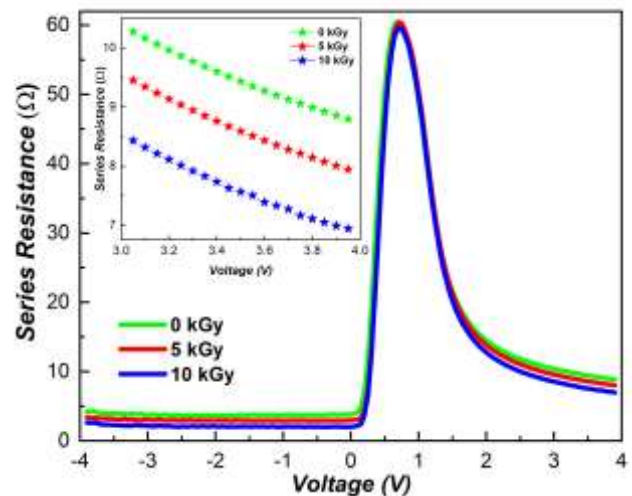


Fig.3. The GaAs-based MIS device's R_i - V curves under radiation.

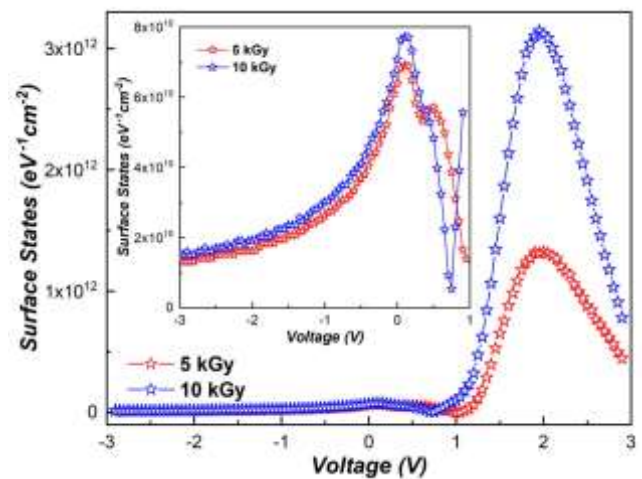


Fig.4. The behaviour of radiation-induced surface states for GaAs-based MIS device.

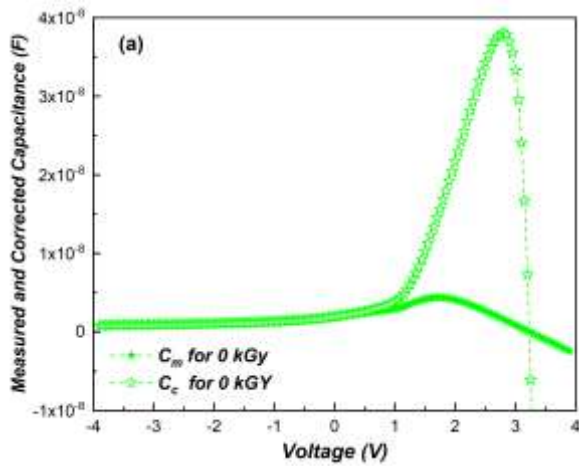


Fig.5a. The Cm-Cc-V graphs of the GaAs-based MIS device for the unirradiated sample.

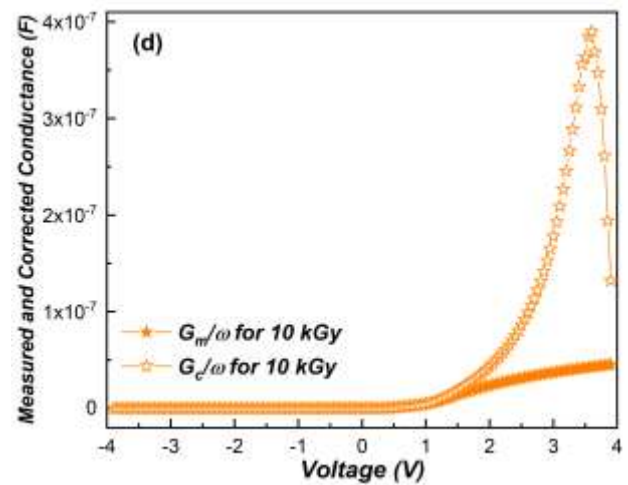


Fig.5d. The Gm/ω-Gc/ω-V graphs of the GaAs-based MIS device after 10 kGy radiation doses.

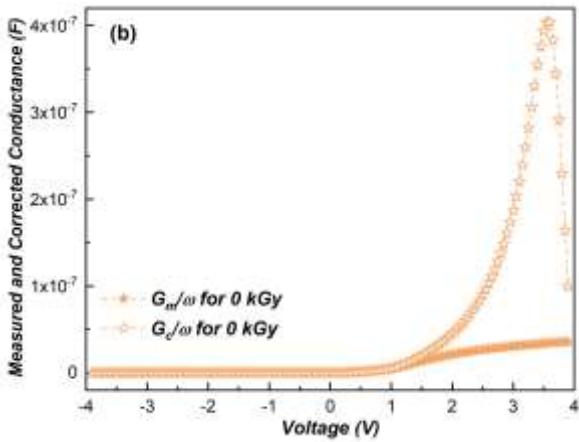


Fig.5b. The Gm/ω-Gc/ω-V graphs of the GaAs-based MIS device for the unirradiated sample.

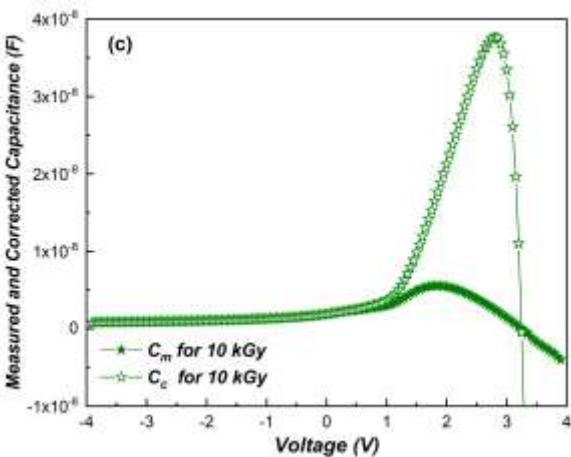


Fig.5c. The Cm-Cc-V graphs of the GaAs-based MIS device after 10 kGy radiation doses.

As shown in Figs. (5a-5d), the capacitance and conductance values increase significantly when the R_s effect is neglected in the positive voltages, and the peak points of the capacitance curves shift towards the positive biases. The $G_c/\omega-V$ features also give a peak before and after irradiation, although there aren't any peaks in the $G_m/\omega-V$ curves. These peaks in $G_c/\omega-V$ properties caused by interface traps indicate that charge transfer can occur via diffusion at the M/S interface (mechanical tunnelling mechanism). Briefly, series resistance can seriously affect the devices' capacitance and conductance characteristics. Furthermore, it can hide the interface trap effects, especially in the depletion region.

When the radiation-induced surface states are examined, it can be seen that they increase depending on the radiation dose and give a peak of around two volts depending on the voltage biases. In conclusion, the shifts in the capacitance curves and the peaks in conductance curves indicate the changing trap charge density with the gamma-radiation effect. The shifting of the $C_c-G_c/\omega-V$ characteristics compared to the measured $C-G/\omega-V$ curves also indicate charge trapping in the interlayer for the irradiated sample.

The accumulated charges in the interlayer (oxide) result in MIS devices' degradation under ionizing radiation. This degradation is because of the change in silicon dioxide's chemical and physical features as well as the passivation of dangling bonds. The generation of trap centres is also possibly responsible for feature differences [50]. However, when the radiation-induced N_{ss} is examined (at about $3 \times 10^{12} \text{ eV}^{-1} \text{ cm}^{-2}$), it can be seen that its level is not very high for pinning the fermi energy level [50] under the maximum cumulative dose of gamma-irradiation. The level of the R_s is also deficient, and it changes less than 2Ω (from 8.74 to 6.82 Ω) for the maximum radiation doses (10 kGy). Therefore, it is possible to say that the degradation in this MIS device is insignificant, and it can be used as an electronic component in ionizing (gamma) radiation environments with an irradiation dose of around 10 kGy.

IV. CONCLUSION

The C - V graphs of MIS/MOS devices, especially GaAs-based devices, may exhibit negative behaviour or a concave curvature in the high voltage biases. Negative capacitance values indicate that the inductive effect of the device is more pressure than the capacitive effect. In this study, the GaAs-based MIS device (Au/n-GaAs/Au-Ge with natural oxide layer) was produced, and its capacitance and conductance data were obtained for 0 (unirradiated sample), 5 and 10 kGy ionizing (gamma) radiation doses. Thus, this study focuses on the negative capacitance phenomenon of MIS devices under ionizing radiation, and experimental results show that abnormal peaks were observed in C - V graphs, and the peak point shifted toward the positive biases after the device was exposed to gamma irradiation. On the other hand, the conductance values increased rapidly and reached their maximum value, while the capacitance values reached their minimum value in the high voltage biases. This situation is directly related to the MIS devices' inductive behaviour, which was determined to be more effective after irradiation. Such behaviours can be observed because of the ionization process, the MIS devices' series resistance, surface states between the M/S interface, and some displacement damages caused by ionizing radiation.

The actual series resistance values with R_i - V curves, correct capacitance-conductance graphs, and the radiation-induced surface states were also obtained to clarify the effects of radiation on the device. And results show that the capacitance and conductance values increase significantly when the R_s effect is neglected (after the correction process), especially in the positive voltages. The peak points of the capacitance curves shift towards the positive biases. Furthermore, the G/ω - V graphs give a peak before and after irradiation, although there aren't any peaks in the G_m/ω - V curves. Therefore, it can be said that the R_s can seriously affect the devices' capacitance and conductance characteristics.

In conclusion, the radiation-induced surface states changed around $3 \times 10^{12} \text{ eV} \cdot \text{cm}^{-2}$ for the maximum cumulative dose (10 kGy), and the actual resistance values changed to 8.74, 7.88, and 6.82 Ω for 0, 5, and 10 kGy amounts, respectively. Shortly, the degradation rate in the device was found to be negligible. Therefore, this MIS device can be safely used as an electronic component in some radiation environments, such as space, where operating satellite systems, and nuclear plants, at gamma irradiation doses of around 10 kGy.

ACKNOWLEDGEMENT

The author wishes to thank Prof. Dr Şemsettin Altındal and his research team for making it possible to conduct the application parts of this study at Gazi University.

REFERENCES

- [1] S. M. Sze and K. K. Ng, *Physics of Semiconductor Devices*. Hoboken, NJ, USA: John Wiley & Sons, Inc., 2006. doi: 10.1002/0470068329.
- [2] R. L. Boylestad and L. Nashelsky, *Electronic Devices and Circuit Theory*, Eleventh Edition. Harlow: Pearson Education Limited, 2014.
- [3] H. Durmuş, A. Tataroğlu, Ş. Altındal, and M. Yıldırım, "The effect of temperature on the electrical characteristics of Ti/n-GaAs Schottky diodes," *Current Applied Physics*, vol. 44, pp. 85–89, Dec. 2022, doi: 10.1016/j.cap.2022.09.015.
- [4] S. Demirezen, Ş. Altındal, Y. Azizian-Kalandaragh, and A. M. Akbaş, "A comparison of Au/n-Si Schottky diodes (SDs) with/without a nanographite (NG) interfacial layer by considering interlayer, surface states (N_{ss}) and series resistance (R_s) effects," *Phys Scr*, vol. 97, no. 5, p. 055811, May 2022, doi: 10.1088/1402-4896/ac645f.
- [5] A. Kaya, Ş. Altındal, Y. Ş. Asar, and Z. Sönmez, "On the Voltage and Frequency Distribution of Dielectric Properties and ac Electrical Conductivity in Al/SiO₂/p-Si (MOS) Capacitors," *Chinese Physics Letters*, vol. 30, no. 1, p. 017301, Jan. 2013, doi: 10.1088/0256-307X/30/1/017301.
- [6] A. Amiri, "Solid-phase microextraction-based sol-gel technique," *TrAC Trends in Analytical Chemistry*, vol. 75, pp. 57–74, Jan. 2016, doi: 10.1016/j.trac.2015.10.003.
- [7] B. Akin, J. Farazin, Ş. Altındal, and Y. Azizian-Kalandaragh, "A comparison electric-dielectric features of Al/p-Si (MS) and Al/(Al₂O₃:PVP)/p-Si (MPS) structures using voltage-current (V - I) and frequency-impedance (f - Z) measurements," *Journal of Materials Science: Materials in Electronics*, vol. 33, no. 27, pp. 21963–21975, Sep. 2022, doi: 10.1007/s10854-022-08984-2.
- [8] K. Choy, "Chemical vapour deposition of coatings," *Prog Mater Sci*, vol. 48, no. 2, pp. 57–170, 2003, doi: 10.1016/S0079-6425(01)00009-3.
- [9] R. Asmatulu, "Highly Hydrophilic Electrospun Polyacrylonitrile/Polyvinylpyrrolidone Nanofibers Incorporated with Gentamicin as Filter Medium for Dam Water and Wastewater Treatment," *Journal of Membrane and Separation Technology*, vol. 5, no. 2, pp. 38–56, Jul. 2016, doi: 10.6000/1929-6037.2016.05.02.1.
- [10] H. E. Lapa, A. Kökce, A. F. Özdemir, and Ş. Altındal, "Investigation of Dielectric Properties, Electric Modulus and Conductivity of the Au/Zn-Doped PVA/n-4H-SiC (MPS) Structure Using Impedance Spectroscopy Method," *Zeitschrift für Physikalische Chemie*, vol. 234, no. 3, pp. 505–516, Mar. 2020, doi: 10.1515/zpch-2017-1091.
- [11] H. Zhou and S. F. Bent, "Fabrication of organic interfacial layers by molecular layer deposition: Present status and future opportunities," *Journal of Vacuum Science & Technology A: Vacuum, Surfaces, and Films*, vol. 31, no. 4, p. 040801, Jul. 2013, doi: 10.1116/1.4804609.
- [12] A. Mishra, N. Bhatt, and A. K. Bajpai, "Nanostructured superhydrophobic coatings for solar panel applications," in *Nanomaterials-Based Coatings*, Elsevier, 2019, pp. 397–424. doi: 10.1016/B978-0-12-815884-5.00012-0.
- [13] H. Sawatari and O. Oda, "Schottky diodes on n -type InP with CdOx interfacial layers grown by the adsorption and oxidation method," *J Appl Phys*, vol. 72, no. 10, pp. 5004–5006, Nov. 1992, doi: 10.1063/1.352027.
- [14] A. Kaymaz, "Ionizing radiation response of bismuth titanate-based metal-ferroelectric-semiconductor (MFS) type capacitor," *Microelectronics Reliability*, vol. 133, p. 114546, Jun. 2022, doi: 10.1016/j.microrel.2022.114546.
- [15] S. Demirezen, A. Kaya, Ş. Altındal, and İ. Uslu, "The energy density distribution profile of interface traps and their relaxation times and capture cross sections of Au/GO-doped PrBaCoO nanoceramic/n-Si capacitors at room temperature," *Polymer Bulletin*, vol. 74, no. 9, pp. 3765–3781, Sep. 2017, doi: 10.1007/s00289-017-1925-2.
- [16] A. Kaymaz, H. Uslu Tecimer, E. Evcin Baydilli, and Ş. Altındal, "Investigation of gamma-irradiation effects on electrical characteristics of Al/(ZnO-PVA)/p-Si Schottky diodes using capacitance and conductance measurements," *Journal of Materials Science: Materials in Electronics*, vol. 31, no. 11, pp. 8349–8358, Jun. 2020, doi: 10.1007/s10854-020-03370-2.
- [17] I. Orak, A. Kocyyigit, and Ş. Alındal, "Electrical and dielectric characterization of Au/ZnO/n-Si device depending frequency and voltage," *Chinese Physics B*, vol. 26, no. 2, p. 028102, Feb. 2017, doi: 10.1088/1674-1056/26/2/028102.
- [18] M. Ambrico *et al.*, "A study of remote plasma nitrided nGaAs/Au Schottky barrier," *Solid State Electron*, vol. 49, no. 3, pp. 413–419, Mar. 2005, doi: 10.1016/j.sse.2004.11.007.
- [19] H. Durmuş, M. Yıldırım, and Ş. Altındal, "On the possible conduction mechanisms in Rhenium/n-GaAs Schottky barrier diodes fabricated by pulsed laser deposition in temperature range of 60–400 K," *Journal of Materials Science: Materials in Electronics*, vol. 30, no. 9, pp. 9029–9037, May 2019, doi: 10.1007/s10854-019-01233-z.
- [20] M. K. Hudait, P. Venkateswarlu, and S. B. Krupanidhi, "Electrical transport characteristics of Au/n-GaAs Schottky diodes on n-Ge at low temperatures," *Solid State Electron*, vol. 45, no. 1, pp. 133–141, Jan. 2001, doi: 10.1016/S0038-1101(00)00230-6.

- [21] D. Ahmad Fauzi, N. K. Alang Md Rashid, M. R. Mohamed Zin, and N. F. Hasbullah, "Radiation Performance of GaN and InAs/GaAs Quantum Dot Based Devices Subjected to Neutron Radiation," *IJUM Engineering Journal*, vol. 18, no. 1, pp. 101–109, May 2017, doi: 10.31436/ijumej.v18i1.653.
- [22] V. Balasubramani, P. v. Pham, A. Ibrahim, J. Hakami, M. Z. Ansari, and T. K. Le, "Enhanced photosensitive of Schottky diodes using SrO interfaced layer in MIS structure for optoelectronic applications," *Opt Mater (Amst)*, vol. 129, p. 112449, Jul. 2022, doi: 10.1016/j.optmat.2022.112449.
- [23] Ş. Karataş, Ş. Altındal, M. Ulusoy, Y. Azizian-Kalendaragh, and S. Özçelik, "Temperature dependence of electrical characteristics and interface state densities of Au/n-type Si structures with SnS doped PVC interface," *Phys Scr*, vol. 97, no. 9, p. 095816, Sep. 2022, doi: 10.1088/1402-4896/ac89bb.
- [24] A. B. Ulsan, A. Tataroglu, Ş. Altındal, and Y. Azizian-Kalendaragh, "Photoresponse characteristics of Au/(CoFe2O4-PVP)/n-Si/Au (MPS) diode," *Journal of Materials Science: Materials in Electronics*, vol. 32, no. 12, pp. 15732–15739, Jun. 2021, doi: 10.1007/s10854-021-06124-w.
- [25] J. R. Nicholls, "Electron trapping effects in SiC Schottky diodes: Review and comment," *Microelectronics Reliability*, vol. 127, p. 114386, Dec. 2021, doi: 10.1016/j.microrel.2021.114386.
- [26] R. M. Sahani and A. Dixit, "A comprehensive review on zinc oxide bulk and nano-structured materials for ionizing radiation detection and measurement applications," *Mater Sci Semicond Process*, vol. 151, p. 107040, Nov. 2022, doi: 10.1016/j.mssp.2022.107040.
- [27] S. Demirezen *et al.*, "Electrical characteristics and photosensing properties of Al/symmetrical CuPc/p-Si photodiodes," *Journal of Materials Science: Materials in Electronics*, Aug. 2022, doi: 10.1007/s10854-022-08906-2.
- [28] A. Tataroglu, Ş. Altındal, M. H. Bölükdemir, and G. Tanır, "Irradiation effect on dielectric properties and electrical conductivity of Au/SiO2/n-Si (MOS) structures," *Nucl Instrum Methods Phys Res B*, vol. 264, no. 1, pp. 73–78, Nov. 2007, doi: 10.1016/j.nimb.2007.07.026.
- [29] Ç. Ş. Güçlü, A. F. Özdemir, A. Karabulut, A. Kökce, and Ş. Altındal, "Investigation of temperature dependent negative capacitance in the forward bias C-V characteristics of (Au/Ti)/Al2O3/n-GaAs Schottky barrier diodes (SBDs)," *Mater Sci Semicond Process*, vol. 89, pp. 26–31, Jan. 2019, doi: 10.1016/j.mssp.2018.08.019.
- [30] E. Arslan, Y. Şafak, Ş. Altındal, Ö. Kelekçi, and E. Özbay, "Temperature dependent negative capacitance behavior in (Ni/Au)/AlGaIn/GaN heterostructures," *J Non Cryst Solids*, vol. 356, no. 20–22, pp. 1006–1011, May 2010, doi: 10.1016/j.jnoncrysol.2010.01.024.
- [31] E. E. Tanrikulu, S. Demirezen, Ş. Altındal, and İ. Uslu, "On the anomalous peak and negative capacitance in the capacitance-voltage (C-V) plots of Al(%7 Zn-PVA)/p-Si (MPS) structure," *Journal of Materials Science: Materials in Electronics*, vol. 29, no. 4, pp. 2890–2898, Feb. 2018, doi: 10.1007/s10854-017-8219-1.
- [32] J. A. M. ALSMAEL, N. URGUN, S. O. TAN, and H. TECİMER, 'Effectuality of the Frequency Levels on the C&w/G/w-V Data of the Polymer Interlayered Metal-Semiconductor Structure', *Gazi University Journal of Science Part A: Engineering and Innovation*, vol. 9, no. 4, pp. 554–561, Dec. 2022, doi: 10.54287/gujssa.1206332.
- [33] S. Demirezen, E. E. Tanrikulu, and Ş. Altındal, "The study on negative dielectric properties of Al/PVA (Zn-doped)/p-Si (MPS) capacitors," *Indian Journal of Physics*, vol. 93, no. 6, pp. 739–747, Jun. 2019, doi: 10.1007/s12648-018-1355-5.
- [34] J. C. Wong and S. Salahuddin, 'Negative Capacitance Transistors', *Proceedings of the IEEE*, vol. 107, no. 1, pp. 49–62, Jan. 2019, doi: 10.1109/JPROC.2018.2884518.
- [35] S. Demirezen, E. E. Tanrikulu, and Ş. Altındal, 'The study on negative dielectric properties of Al/PVA (Zn-doped)/p-Si (MPS) capacitors', *Indian Journal of Physics*, vol. 93, no. 6, pp. 739–747, Jun. 2019, doi: 10.1007/s12648-018-1355-5.
- [36] J. R. Srour and J. W. Palko, "Displacement damage effects in irradiated semiconductor devices," *IEEE Trans Nucl Sci*, vol. 60, no. 3, pp. 1740–1766, 2013, doi: 10.1109/TNS.2013.2261316.
- [37] A. F. Özdemir *et al.*, "The analysis of hydrostatic pressure dependence of the Au/native oxide layer/n-GaAs/Au-Ge Schottky diode parameters," *The European Physical Journal Applied Physics*, vol. 60, no. 1, p. 10101, Oct. 2012, doi: 10.1051/epjap/2012110483.
- [38] A. Kaymaz, E. Evcin Baydilli, H. Uslu Tecimer, Ş. Altındal, and Y. Azizian-Kalendaragh, "Evaluation of gamma-irradiation effects on the electrical properties of Al/(ZnO-PVA)/p-Si type Schottky diodes using current-voltage measurements," *Radiation Physics and Chemistry*, vol. 183, p. 109430, Jun. 2021, doi: 10.1016/j.radphyschem.2021.109430.
- [39] H. G. Çetinkaya, M. Yıldırım, P. Durmuş, and Ş. Altındal, "Diode-to-diode variation in dielectric parameters of identically prepared metal-ferroelectric-semiconductor structures," *J Alloys Compd*, vol. 728, pp. 896–901, Dec. 2017, doi: 10.1016/j.jallcom.2017.09.030.
- [40] S. Demirezen, H. G. Çetinkaya, and Ş. Altındal, "Doping rate, Interface states and Polarization Effects on Dielectric Properties, Electric Modulus, and AC Conductivity in PCBM/NiO:ZnO/p-Si Structures in Wide Frequency Range," *Silicon*, Jan. 2022, doi: 10.1007/s12633-021-01640-0.
- [41] B. Rong, L. K. Nanver, J. N. Burghartz, A. B. M. Jansman, A. G. R. Evans, and B. S. Rejaei, "C-V characterization of MOS capacitors on high resistivity silicon substrate," in *Electrical Performance of Electrical Packaging (IEEE Cat. No. 03TH8710)*, pp. 489–492, doi: 10.1109/ESSDERC.2003.1256920.
- [42] M. Ulusoy, Ş. Altındal, Y. Azizian-Kalendaragh, S. Özçelik, and Z. Mirzaei-Kalar, "The electrical characteristic of an MIS structure with biocompatible minerals doped (Brushite+Monetite: PVC) interface layer," *Microelectron Eng*, vol. 258, p. 111768, Apr. 2022, doi: 10.1016/j.mee.2022.111768.
- [43] Ş. Altındal and H. Uslu, "The origin of anomalous peak and negative capacitance in the forward bias capacitance-voltage characteristics of Au/PVA/n-Si structures," *J Appl Phys*, vol. 109, no. 7, p. 074503, Apr. 2011, doi: 10.1063/1.3554479.
- [44] Ç. Bilkan and Ş. Altındal, "Investigation of the C-V characteristics that provides linearity in a large reverse bias region and the effects of series resistance, surface states and interlayer in Au/n-Si/Ag diodes," *J Alloys Compd*, vol. 708, pp. 464–469, Jun. 2017, doi: 10.1016/j.jallcom.2017.03.013.
- [45] J. R. Srour, C. J. Marshall, and P. W. Marshall, "Review of displacement damage effects in silicon devices," *IEEE Trans Nucl Sci*, vol. 50, no. 3, pp. 653–670, Jun. 2003, doi: 10.1109/TNS.2003.813197.
- [46] E. H. Nicollian and J. R. Brews, *MOS (Metal Oxide Semiconductor) Physics and Technology*. Hoboken, NJ: Wiley, 2003.
- [47] A. Teffahi *et al.*, "Effect of 60Co γ -ray irradiation on electrical properties of Ti/Au/GaAs1-xNx Schottky diodes," *Current Applied Physics*, vol. 16, no. 8, pp. 850–858, Aug. 2016, doi: 10.1016/j.cap.2016.05.003.
- [48] S. Kaya, A. Aktag, and E. Yilmaz, "Effects of gamma-ray irradiation on interface states and series-resistance characteristics of BiFeO3 MOS capacitors," *Nucl Instrum Methods Phys Res B*, vol. 319, pp. 44–47, Jan. 2014, doi: 10.1016/j.nimb.2013.11.006.
- [49] Ş. Karataş, A. Türüt, and Ş. Altındal, "Irradiation effects on the C-V and G/w-V characteristics of Sn/p-Si (MS) structures," *Radiation Physics and Chemistry*, vol. 78, no. 2, pp. 130–134, Feb. 2009, doi: 10.1016/j.radphyschem.2008.09.006.
- [50] R. Castagné and A. Vapaille, 'Description of the SiO2-Si interface properties by means of very low frequency MOS capacitance measurements', *Surf Sci*, vol. 28, no. 1, pp. 157–193, Nov. 1971, doi: 10.1016/0039-6028(71)90092-6.
- [51] S. Maurya and S. Awasthi, "Effect of zero bias, 2.7 MeV proton irradiation on HfO2," *J Radioanal Nucl Chem*, vol. 318, no. 2, pp. 947–953, Nov. 2018, doi: 10.1007/s10967-018-6229-y.

BIOGRAPHIES



AHMET KAYMAZ received the B.S. degree in electrical and electronics engineering from Pamukkale University, Denizli, in 2006. He also received his M.S. and Ph.D. in electrical and electronics engineering from Karabuk University, Karabuk, Turkey, in 2015 and 2020, respectively. From

2010 to 2020, he was a Research Assistant at Karabuk University. Since 2020, he has worked as an Assistant Professor at Karabuk University, Engineering Faculty, Department of Mechatronics Engineering.